I. Project Research

Project 12

PR12 Improvement of Characterization Techinques in High-Energy-Particle Irradiation Research

A. Kinomura

Research Reactor Institute, Kyoto University

OBJECTIVES: Irradiation facilities of high-energy particles for neutrons (Material Controlled irradiation Facility), ions (e.g., Heavy ion irradiation facility) and electrons (Low temperature irradiation facility, KUR-LINAC) have been extensively developed at the Research Reactor Institute. The developed facilities have been in operation and opened for joint research projects. One of the objectives of this project is to improve or optimize irradiation facilities for more accurate irradiation experiments.

As characterization techniques for irradiated materials, a slow positron-beam system and a focused ion beam system have been developed and introduced, respectively, in addition to previous characterization facilities such as an electron microscope, an electron-spin-resonance spectrometer, a bulk positron annihilation spectrometer and a thermal desorption spectrometer. Another objective is to introduce new techniques or reconsider analytical methods of previously used characterization techniques.

Based on these two objectives, we expect promotion of previous research and attraction of new users for the joint research program. The allotted research subject (ARS) and individual co-researchers are listed below.

ARS-1:
Study on efficient use of positron moderation materials (A. Kinomura *et al.*)

ARS-2:
Effects of electron-irradiation on Cu solubility and diffusivity in Fe studied by three dimensional atom probe (K. Nagumo *et al.*)

ARS-3:
Irradiation defects of F82H irradiated at SINQ using positron annihilation spectroscopy (K. Sato *et al.*)

ARS-4:
Study on irradiation effect and electrical and optical properties of compound semiconductors (K. Kuriyama *et al.*)

ARS-5:
Validation of D3×t0.5 TEM disk size miniature test specimens for post-irradiation thermal diffusivity measurement (M. Akiyoshi and A. Kinomura)

ARS-6:
Positron annihilation study on Fe-Cr binary alloy after electron irradiation (T. Onitsuka *et al.*)

ARS-7:
Positron annihilation study on free-spaces in DLC and heteroelement-containing DLC films (K. Kanda *et al.*)

ARS-8
Thermal stability of diamond-like carbon films (S. Nakao *et al.*)

RESULTS: In ARS-1, the performance of the brightness enhancement system of the slow positron-beam system of Kyoto University research Reactor (KUR) was evaluated by using an electron beam instead of a positron beam with emphasis on focused beam sizes as function of extraction coil current.

In ARS-2, a sample holder for temperature-controlled electron irradiation by KURRI-LINAC has been developed to investigate radiation-enhanced diffusion processes of impurity atoms in Fe. The experiments indicated that the dissipation of beam heat is important to control irradiation temperatures.

In ARS-3, reduced activation ferritic martensitic (RAFM) steels irradiated by a spallation neutron source and an electron beam were compared to investigate the He effects on irradiation-induced defects. Positron annihilation coincidence Doppler broadening (CDB) measurements were performed to characterize the samples.

In ARS-4, GaN samples after gamma-ray irradiation to a total absorption dose of 160 kGy were characterized by Rutherford backscattering spectrometry using a 1.5 MeV proton beam to investigate the effect of gamma-rays during transmutation doping by neutron irradiation.

In ARS-5, TEM disk size miniature test specimens to investigate the influence of irradiation on thermal diffusivity was examined by 8 MeV electron beam irradiation using KURRI-LINAC. It is concluded that the use of miniature specimens is validated.

In ARS-6, simple binary Fe-40Cr alloy samples after 9 MeV electron irradiation by KURRI-LINAC were characterized by positron annihilation lifetime spectroscopy and positron annihilation coincidence Doppler broadening (CDB) measurement.

In ARS-7, positron annihilation lifetime measurements for DLC films by a slow positron beam were planned but no experiment was performed as KUR was not in operation.

In ARS-8, the relationship between thermal stability and the bonded hydrogen in several types of DLC films by thermal desorption spectroscopy (TDS). The results indicated that the structural changes may be driven by the creation and annihilation of defects caused by hydrogen desorption.

CONCLUSION: Developments and improvements on the slow positron-beam system and electron irradiation have been performed. Combinations of new materials and different irradiation/characterization techniques have been examined. These studies were performed in the line of the two objectives in this project. Further studies are expected in the following year.

PR12-1 # Study on Efficient Use of Positron Moderation Materials

A. Kinomura, N. Oshima[1] and A. Yabuuchi

Research Reactor Institute, Kyoto University
[1]National Institute of Advanced Industrial Science and Technology (AIST)

INTRODUCTION: Positron annihilation spectroscopy is widely known as a method to probe vacancies, vacant spaces and free volume of atomic scales. It is considerably important to obtain intense and mono-energetic slow positron beams to perform positron annihilation spectroscopy of thin films or surface layers. Positron sources based on pair creation can generate more intense slow positron beam than radioisotope-based positron sources. Therefore, positron sources using pair-creation by gamma-rays from a nuclear reactor have been developed to obtain an intense slow positron beam at Kyoto University Research Reactor Institute. Sizes of reactor-based positron sources are generally wider than accelerator-based sources. In the case of the slow positron beam system at Kyoto University research Reactor (KUR), the size of the positron source is approximately 30 mm in diameter. As sample sizes of actual samples are often less than 10 mm, it is necessary to reduce beam sizes efficiently with keeping beam intensity as high as possible. For positron beams differently with electron beam, brightness enhancement methods are used for this purpose, where strong focusing and efficient positron re-moderation are essential. In this study, we concentrate on the brightness enhancement system in the KUR slow positron beam system.

EXPERIMENTS: Electron beams have been used as an alternative methods. Two types of electron sources were prepared for this study. They are a photoelectric source using ultraviolet light illumination and a thermal electron source using a filament. The photoelectron source is used for weak beam measurements comparable with positron sources. The thermal electron source is used for transport efficiency measurements with relatively intensive beams that can be detected by an ammeter. For both methods, phosphor screens with microchannel plates were used to monitor beam shapes.

Focusing performance of the brightness enhancement system was evaluated with the electron beams. Figure 1 shows the schematic view of the brightness enhancement system of the KUR slow positron beam system [1]. Positrons (electrons) are transported by guiding magnetics fields by solenoid and Helmholtz coils along the beamline. However, the beam has to be extracted from the guiding magnetic fields for focusing using magnetic lens as the guiding magnetic fields interfere with the focusing magnetic field. The termination of guiding magnetic fields is achieved by gradually reducing and/or inverting magnetic fields. In Fig. 1, large Helmholtz coils were used for transport magnetic fields and smaller Helmholtz coils (labelled as MA and MB) were used to adjust the termination fields.

RESULTS: To examine and optimize the beam extraction method from the guiding magnetic field to the focusing magnetic field, beam diameters were measured as a function of extraction coil (MA in Fig. 1) current in Fig. 2. The second extraction coil (MB) was not used in this case. The electron energy at the source was 10 eV and the acceleration energy at the acceleration gap (‘accel. gap’ in Fig. 1) was 5 keV. Beam trajectory calculations indicated that the beam divergence at the lens entrance increase with increasing lens current (not shown). The simulation also indicated that the focusing properties of the lens is non-linear and focusing is stronger with increasing radial distance from the beam axis. On the other hand, the influence of spherical aberration gets more significant with increasing radial distance. The variation of the beam diameter in Fig. 2 can be interpreted as a result of combination of the two effects. Thus, optimum extraction coil current must be carefully determined.

In summary, we have evaluated performance of the brightness enhancement system of the KUR slow positron beam system by using an electron beam instead of a positron beam. In particular, the beam extraction from the guiding magnetic field was examined as function of the extraction coil current.

ACKNOWLEDGEMENT: We would like to acknowledge the important contribution of Yoshihiro Kuzuya on this study.

REFERENCE:

[1] Y. Kuzuya *et al.* J. Phys. Conf. Series 791 (2017) 012012.

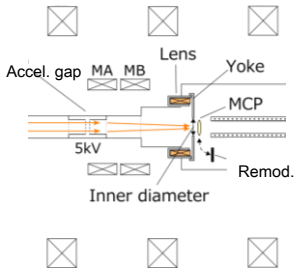

Fig. 1. Schematic view of the Helmholtz coils around the brightness enhancement system.

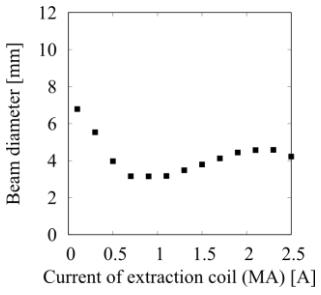

Fig. 2. Beam diameter as a function extraction-coil current at the re-moderator position.

PR12-2 Effects of Electron-irradiation on Cu Solubility and Diffusivity in Fe Studied by Three Dimensional Atom Probe

K. Nagumo, Y. Nagai, K. Inoue, T. Toyama, Y. Shimizu, B. Han, M. Shimodaira, A. Kimomura[1], T. Yoshiie[1], Q. Xu[1], A. Yabuuchi[1]

Institute for Materials Research, Tohoku University
[1]Research Reactor Institute, Kyoto University

INTRODUCTION: Reactor pressure vessel (RPV) is one of the most important parts in nuclear power plant since RPV holds nuclear fuels, control rods and primary cooling water. Therefore, irradiation-induced embrittlement of RPV steels is vital issue for the safe operation of nuclear power plants. Substantial studies have revealed that nano-sized Cu precipitates are formed by neutron-irradiation and cause the embrittlement. In order to understand the kinetics of Cu precipitation, the diffusion coefficient and the solubility limit of Cu in Fe are the important basic quantities [1, 2].

It is predicted that diffusivity and solubility may be strongly affected by irradiation [3]; for example, diffusivity is greatly enhanced by irradiation because vacancies and interstitials, which are necessary for diffusion of solute atoms, are remarkably induced during irradiation. Such enhancement of diffusion has been modeled and simulated, however, experimental studies are very limited at present. In this study, we introduce Frenkel pair which can evaluate basic irradiation effect using KUR LINAC, and try to investigate the electron-irradiation effects on Cu diffusivity in Fe. In addition, the electron-irradiation effects on the solubility limit is investigated.

EXPERIMENTS: Pure Fe (99.999%) was used as a base material for the sample. It was cut into a plate shape of about 5 mm × 5 mm × 1 mm and the surface of the sample was mechanically polished with abrasive papers of #2000. After removal of the machined layer by chemical polishing, the sample was evacuated to 10^{-5} Pa or less. Further, Ar gas sputtering was performed in the vacuum chamber to clean the sample surface. Pure Cu (99.999%) was used as the deposition source after chemical polishing with 5% nitric acid to remove the oxide layer on the surface. In the vacuum chamber, electron-beam heating was employed for dissolution of Cu. The deposition thickness of Cu on Fe was ~3 μm, which was sufficient for the diffusion distance (several 100 nm) expected in this experiment.

Electron-irradiation was performed with electron beam with energy of 5 MeV at LINAC. The irradiation temperature and the irradiation time were about 700 K and 30000 seconds, respectively.

After electron-irradiation, needle-like samples containing a copper-iron interface for three-dimensional atom probe (3D-AP) were fabricated with focused-ion beam apparatus. In 3D-AP measurement, a laser pulse mode was employed to reduce the frequency of sample fracture, at temperature of 55 K, a laser energy of 100 pJ, and a repetition frequency of 200 kHz.

RESULTS: Figure 1 shows atom maps of Cu, Fe and O in the electron-irradiated Cu-Fe diffusion pair. The interface of Cu-Fe was successfully detected. Cu atoms were hardly observed in Fe matrix region, and its concentration was less than 0.04 in atomic percent. 3D-AP measurements were performed by using several needle-like samples, and the similar results to fig. 1 were obtained. It is noted that O, a typical impurity of this system, was not segregated at the Cu-Fe interface nor penetrated into Fe matrix, showing no impact of such impurities on Cu mobility.

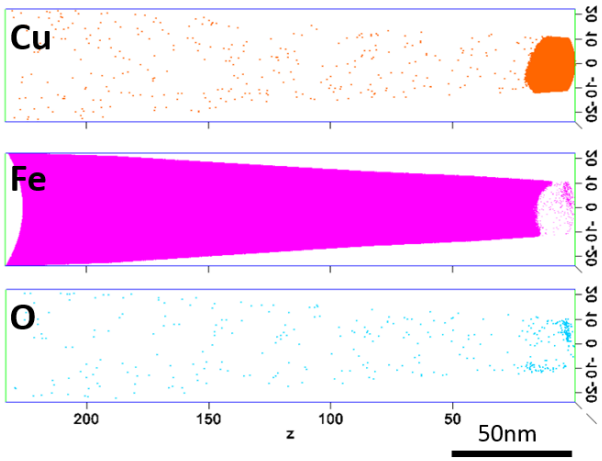

Fig. 1: Atom map obtained by 3D-AP analysis for Cu and Fe in Cu-Fe diffusion pair electron irradiated at LINAC in KUR at 700 K for 30000 seconds.

The obtained 3D-AP results show that the solubility limit of Cu in Fe hardly changes even under electron-irradiation. On the other words, it was found that forced solid solution due to excessive atomic vacancies did not occur.

In order to clarify the irradiation effect against diffusion, we plan to evaluate the diffusion coefficient of Cu via the kinetics of Cu precipitation by conducting similar irradiation experiments on Fe-Cu dilute alloy, such as water-quenched Fe-1.0wt. %Cu alloy.

REFERENCES:

[1] T. Toyama *et al.*, Scrip. Mater., **83** (2014) 5-8.
[2] M. Shimodaira *et al.*, Mater. Trans., **9** (2015) 1513-1516.
[3] R. Sizmann, J. Nucl. Mater., **69**&**70** (1968) 386-412.

PR12-3 Irradiation Defects of F82H Irradiated at SINQ Using Positron Annihilation Spectroscopy

K. Sato, K. Ikemura[1], V. Krsjak[2], C. Vieh[2], R. Brun[2], Q. Xu[1], T. Yoshiie[1] and Y. Dai[2]

Graduate School of Science and Engineering, Kagoshima University

[1] Research Reactor Institute, Kyoto University
[2] Spallation Neutron Source Division, Paul Scherrer Institut

INTRODUCTION: The reduced activation ferritic/martensitic (RAFM) steels are candidates for the first wall and blanket of fusion reactors [1]. Because of its good irradiation resistance, the study of irradiation effects of the RAFM steels is also important for the structural materials of spallation neutron source including accelerator driven system [2]. One of features of spallation neutron source is high production rate of gas atoms [3], which leads to the formation of a large amount of He bubbles. He bubbles have great influence on mechanical properties of structural materials [4,5], and clarifying the growth mechanism of He bubbles is significant for the development of nuclear materials. In the present study, the defect structures in F82H irradiated with protons and neutrons by SINQ (the Swiss Spallation Nuetron Source) were studied using positron annihilation spectroscopy, and the growth process of He filled vacancy clusters by the isochronal annealing test was discussed.

EXPERIMENTS: The F82H was irradiated in the second STIP (STIP-II, the SINQ target irradiation program). The irradiation dose, average irradiation temperature, and calculated production of H and He were 7.2 dpa, 385 K, 531.5 appm and 2105 appm, respectively. For comparison, 8 MeV electron irradiation was also performed for 5.5 h (short term, 7.23×10^{21} e^-/m^2, 1.3×10^{-4} dpa) and for 70 h (long term, 9.29×10^{22} e^-/m^2, 1.7×10^{-3} dpa). A three-detector system using a fast digital oscilloscope [6] was adopted for the positron annihilation lifetime (PAL) measurements, thereby reducing the background counts and making it possible to measure highly radioactive samples. The time resolution of the system was 150 ps (full width at half maximum). Each spectrum was accumulated to a total of 1.4×10^6 counts. The spectra were analyzed using the PALSfit program [7]. Positron annihilation coincidence Doppler broadening (CDB) measurements were also performed. In order to obtain CDB spectra, two Ge-detectors were placed at 180° with respect to one another with a spacing of about 400 mm therebetween. The overall energy resolution of the two Ge-detectors was 1.4 keV at FWHM for 511 keV γ–rays. CDB spectra were accumulated to a total of more than 1.0×10^7 counts. Sabelova et al. reported that He effect range of CDB spectra is $5-12 \times 10^{-3}$ mc [8]. Therefore, the parameters S and W are defined as the ratio of the low-momentum ($|P_L| < 2.5\times10^{-3}$ mc) and high-momentum (7×10^{-3} $mc < |P_L| < 12 \times 10^{-3}$ mc) areas in the Doppler-broadening spectrum to the total area, respectively. Here, m is the electron rest mass and c is the velocity of light.

RESULTS: Variation in S-parameter is almost the same as that in mean positron lifetime. This correspondence between S-parameter and mean lifetime was also obtained in the previous study [9]. The long lifetime decreases as the annealing temperature is increased up to 573 K, and the spectrum does not decompose into two components after annealing at 673 K. The lifetime decrease is due to the absorption of He atoms weakly trapped in the matrix. The increase of the mean lifetime above 873 K results from the growth of He bubbles by absorption of vacancies and the release of H atoms. The vacancy (V)-He_n complexes dissociate at 773 K and the release of H atoms from proton and spallation neutron-irradiated F82H peaks between 573 and 673 K. We cannot see the conspicuous peak caused by the He atoms in the momentum range of $5-12 \times 10^{-3}$ mc in CDB ratio curves. In order to get the He effect on the CDB spectra, S–W plots were drawn. Maximum error of S and W parameters is 2.5×10^{-4} and 1.2×10^{-4}, respectively. In the electron irradiation, only defects are introduced and gas atoms are not formed. Positron trapping rate into He bubbles is smaller than that into empty voids. So, if CDB spectra are influenced by the He atoms of He filled vacancy clusters, the change in S- and W-parameter should be different from that of electron-irradiated samples. The slope is slightly different between solid and broken line, and this difference means the effect of He atoms.

REFERENCES:

[1] M. Tamura *et al.*, J. Nucl. Mater. 141 (1986) 1067.
[2] Y. Dai and G.S. Bauer, J. Nucl. Mater. 296 (2001) 43.
[3] Y. Dai *et al.*, J. Nucl. Mater. 343 (2005) 33.
[4] Z. Tong and Y. Dai, J. Nucl. Mater. 385 (2009) 258.
[5] Z. Tong and Y. Dai, J. Nucl. Mater. 398 (2010) 43.
[6] H. Saito *et al.*, Nucl. Instr. Meth. Phys. Res. A 487 (2002) 612.
[7] J.V. Olsen *et al.*, Phys. Status Solidi C 4 (2007) 4004.
[8] V. Sabelova *et al.*, J. Nucl. Mater. 450 (2014) 54.
[9] V. Krsjak *et al.*, J. Nucl. Mater. 456 (2015) 382.

PR12-4

Study on Irradiation Effect and Electrical and Optical Properties of Compound Semiconductors

K. Kuriyama, N, Nishikata, Y. Torita, K. Kushida[1], A. Yabuuchi[2], Q. Xu[2] and A. Kinomura[2]

College of Engineering and Research Center of Ion Beam Technology, Hosei University
[1]Osaka Kyoiku University
[2]Research Reactor Institute, Kyoto University

INTRODUCTION: Examining the defects caused by various radiations to GaN under the space environment is important. In our previous study [1, 2], we reported that the energy levels relating to nitrogen vacancy (V_N) and gallium vacancy (V_{Ga}) were induced by neutron and proton irradiated GaN. The neutron irradiation has been used as the neutron transmutation doping into semiconductors such as GaAs [3], GaP [4], and GaN [5]. Atoms in semiconductors mainly transmute by a (n, γ) reaction. Therefore, to survey the radiation effect of gamma ray alone is meaningful. In the present study, we report the lattice displacement in GaN bulk single crystals by gamma-ray irradiation.

EXPERIMENTS: GaN bulk single crystals with a thickness of 450 ± 50 μm were purchased from Furukawa Co. Ltd. The crystals were irradiated at room temperature with gamma-rays of 1.17 and 1.33 MeV from a cobalt-60 source of Kyoto University Research Reactor Institute. Samples were irradiated with an absorption dose rate of 1.771 KGy/h. Total gamma-ray dose was 160 kGy. The resistivity varied from 30 Ωcm for an un-irradiated sample to 10^4 Ωcm for gamma-ray irradiated one. Rutherford backscattering spectroscopy analysis (RBS) was carried out using 1.5-MeV H^+ ions from the van de Graaff accelerator of Hosei University.

RESULTS: Fig. 1 shows typical random and aligned RBS spectra of as-irradiated and un-irradiated GaN bulk single crystal. The aligned spectra were obtained from scattering along the <0001> channeling directions. The minimum yield χ_{min} (the ratio between aligned and random) of Ga and N was evaluated using a width of about 20 channels (120 nm) behind the surface peak. The values of χ_{min} for Ga were 1.5 % for un-irradiated and 2.3 % for gamma-ray irradiated samples. On the other hand, the values of χ_{min} for N were 7.7 % for un-irradiated and 9.5 % for gamma-ray irradiated samples. The number of displaced Ga and N atoms estimated using χ_{min} values were 3.5×10^{20} cm^{-3} and 8.7×10^{20} cm^{-3}, respectively. Although the disorder is recognized in Ga and N lattices, the displacement concentration of N atoms is about two times larger than that of Ga atoms. This suggests that N interstitial (N_i) exists in gamma-ray irradiated GaN bulk single crystal. This result is similar to that of the neutron irradiated GaN [6]. Since N_i atoms form the deep acceptor level at 960 meV below the bottom of the conductiones band [6], the origin of the high resistivity after the gamma-ray irradiation is attributed to the carrier compensation effect due to the deep level of N_i.

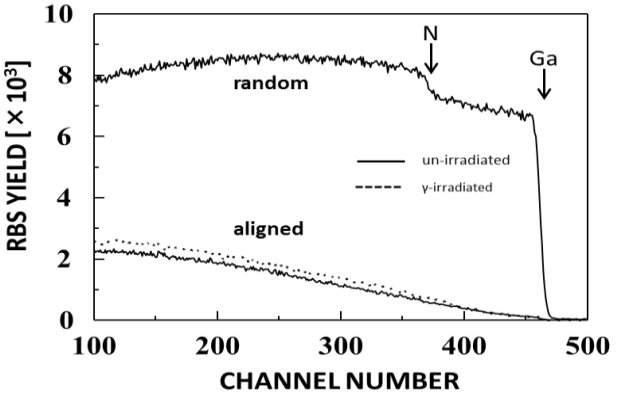

Fig. 1 Random and aligned RBS spectra of un-irradiated and gamma-ray irradiated GaN.

This study has been accepted as Proceedings (Journal of Physics, IOP (UK)) of International Conference on the Physics of Semiconductors 2016 , Beijing.

REFERENCES:

[1] K. Kuriyama, M, Ooi, A. Onoue, K. Kushida, and Q. Xu, Appl. Phys. Lett. 88, 132109 (2006).
[2] T. Nakamura, N. Nishikata, K. Kamioka, K. Kuriyama, and K. Kushida, Nucl. Instrum, Method Phys. Res. B 371, 251 (2016).
[3] M. Satoh, K. Kuriyama, and T. Kawakubo, J. Appl. Phys. 67, 3542 (1990).
[4] K. Kuriyama, Y. Miyamoto, T. Koyama, O. Ogawa, and M. Okada, J. Appl. Phys. 86, 2352 (1999).
[5] K. Kuriyama, T. Tokumasu, J. Takahashi, H. Kondo, and M. Okada, Appl. Phys. Lett. 80, 3328 (2002).
[6] T. Nakamura, K. Kamioka, K. Kuriyama, K. Kushida, Q. Xu, and M. Hasegawa, Sold State Commun.205, 1 (2015).

PR12-5

Validation of D3×t0.5 TEM Disk Size Miniature Test Specimens for Post-irradiation Thermal Diffusivity Measurement

M. Akiyoshi and A. Kinomura[1]

Radiation Research Center, Osaka Prefecture University
[1]Research Reactor Institute, Kyoto University

INTRODUCTION:

Radioactivity levels for conventional thermal diffusivity test specimens are often prohibitively high for handling and measurement outside the hot cell facilities with candidate metallic materials, such as tungsten and reduced activation steels, of near-term technological interest for fusion energy. In addition to this radiological constraint, the steep temperature gradients with specimens due to the high volumetric heating and the extreme cost per volume associated with high flux neutron irradiation in fission reactors strongly incentivize the use of miniaturized test specimens in materials irradiation studies. Therefore, in the ongoing Japan-US PHENIX project, thermal diffusivity measurement is planned to be performed using miniature disc specimens with a diameter (D) of 3mm and a thickness (t) of 0.5mm, which is generally used as specimen disk for TEM. These small specimen dimensions allow a reduction of radioactivity by a factor of 44 as compared with a D10×t2 standard specimen. This study validates this D3×t0.5 miniature specimen type for post-neutron irradiation measurement of thermal diffusivity.

In addition, electron-beam irradiation using KURRI-LINAC is now most effective method to study irradiation effects in thermal diffusivity. It require about one week to achieve 0.01dpa with accelerate energy of 30MeV and highest current (200 μ A) , where the target volume is limited to D10 and thickness was about 2-3 cm. Furthermore, when we using low-energy beam (8MeV) to avoid the activation, it required longer days and thinner target (<1cm). Therefore, the small specimen mentioned above is also important for the electron-beam irradiation.

EXPERIMENTS and RESULTS:

The thermal diffusivity measurements of D3×t0.5 tungsten specimens were performed using a Netzsch LFA-457 from room temperature to 500℃. A specimen holder was designed to fit into a Netzsch standard holder (Fig. 1). Since the back-side of a D3 specimen radiates only a small amount of infrared to measure the temperature change after a laser flash, the extrapolation from the temperature dependency above 150℃ is required to obtain a reliable thermal diffusivity at room temperature. Furthermore, there was still a systematic difference of 20% from a standard size specimen. In the LFA-457 system, the pulse width of laser flash, T_f = 0.33ms, is not fast enough compared with the diffusion time of heat in 0.5mm thickness. It is required that T_f is smaller than 1/10 of $T_{1/2}$, then the thickness of the specimen is required to be larger than 1.3mm for unirradiated tungsten.

Consequently, measurement of the miniature specimens was performed using new Netzsch LFA-467 where the minimum of T_f is only 20μs. Also the LFA-467 uses optics to condense the radiated infrared from a minimum of D3.2mm, therefore exact measurement was achieved for the miniature specimens at room temperature. However, it was turned out that the effect of surface carbon coating is not ignorable to avoid transmission of laser flash and enhance the radiation efficiency of infrared from the back-side. These coating layer is enough thin and the thermal diffusivity is enough high when using D10×t2 standard specimen. On the other hand, the coating layer on the miniature specimen of which thickness is 0.5mm is not ignorable any more. Netzsch Japan developed Graphene-Nanoplatelets spray[1] that resolves this problem. They showed almost same thermal diffusivity between D3×t0.5 miniature specimens and D10×t2 standard specimens, even using β-SiC that shows thermal diffusivity of > 100mm^2/s.

CONCLUSION:

It is concluded that the miniature specimen for measurement of thermal diffusivity is validated and this result will be widely used in future materials irradiation studies.

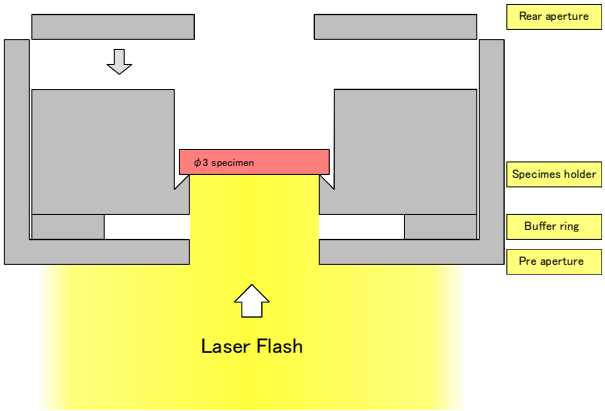

Fig. 1 A schematic image of the specimen holder for D3 small specimens.

REFERENCE:

[1] Y. Ishibashi *et al.*, The 37th Japan Symposium on Thermophysical Properties, Nov.28-30, 2016, Okayama.

PR12-6 Positron Annihilation Study on Fe-Cr binary alloy after Electron Irradiation

T. Onitsuka, K. Sato[1] and Q. Xu[2], J. Kinomura[2] and K. Fukumoto

Research Institute of Nuclear Engineering, Fukui University
[1]Graduate School of Science and Engineering, Kagoshima University
[2]Research Reactor Institute, Kyoto University

INTRODUCTION: High-chromium (9-12%Cr) Ferritic/martensitic steels are attractive candidate material for various nuclear energy systems because of their excellent thermal properties, higher swelling resistance and lower activation compared with conventional austenitic stainless steels. The high-chromium steel as also been considered for both in-core and out-of-core applications of fast breeder reactors, and for the first wall and blanket structures of fusion systems, where irradiation induced degradation is expected to be the critical issues for reactor operation [1]. In this present study, the authors focused on a precipitation response for formation of α'-phase in Fe-Cr binary model alloy subjected to electron irradiation, in order to examine fundamental aspects of radiation effects on α'-phase precipitate development in iron-chromium alloys. The positron annihilation measurement technique was used to study the behaviour of micro-structural evolution due to irradiation-induced defects and the formation of α'-phase simultaneously. Because the phase decomposition into Fe-rich (α) and Cr-rich (α') phases will co-occur in Fe-Cr alloy, the formation of α'-phase precipitates can be detected by positron annihilation coincidence Doppler broadening (CDB) technique owing to a lesser positron affinity for Cr than Fe.

EXPERIMENTS: Simple binary Fe-40Cr alloy was made by arc melting under argon atmosphere in a water-cooled copper hearth. All the ingots were melted and inverted three times in order to promote chemical homogeneities. The obtained ingot was conducted by solution heat treatment at 1077 ℃ for 2 h followed by water quenching, and then, machined to the dimensions of 10 mm × 10 mm × 0.5 mm. 9 MeV electrons irradiated at 100 ℃ in KURRI-LINAC. The irradiation dose and displacement damage range ware 3.0×10^{17}-2.0×10^{18} e/cm^2 and 0.04-0.3 mdpa. After the irradiation, all specimens were mechanically polished and then electrolytically polished with methanol : sulfuric acid = 75 : 25 (Vol. %) at 20-30V to remove surface damage from previous steps. Then, positron annihilation lifetime measurement and CDB measurement were performed.

RESULTS: Fig. 1. shows the positron annihilation lifetime measurement results of electron irradiated Fe-40Cr alloy. The longer lifetime components (τ_2) around 150 psec corresponds to vacancy type defects. They are slightly smaller than the corresponding lifetimes at single vacancy in pure Fe. Fig. 2 shows the S-W plots obtained from positron CDB measurements for the Fe-40Cr alloy before (WQ) and after (0.04-0.3 mdpa) the irradiation. In general, positron trapping in vacancies results in an increase (decrease) in the S- (W-) parameter, since the annihilation with the low-momentum valence electrons increased at the vacancies. A high concentration of defects, or an increase in the mean size of defects leads to a larger contribution of annihilations from low momentum electrons because positrons are trapped at defects. This is reflected in CDB measurements by an increase in the S-parameter and a decrease in the W-parameter as irradiation dose is increased. However a rapid and significant decrease of the S-parameter comparable with a rapid and significant increase of the W-parameter respectively observed between 0.1 mdpa and 0.2 mdpa. This behaviour of the S- and the W- parameters suggests that an abrupt change in the very earliest stage of mocrostructural evolution was detected by positron CDB measurement technique.

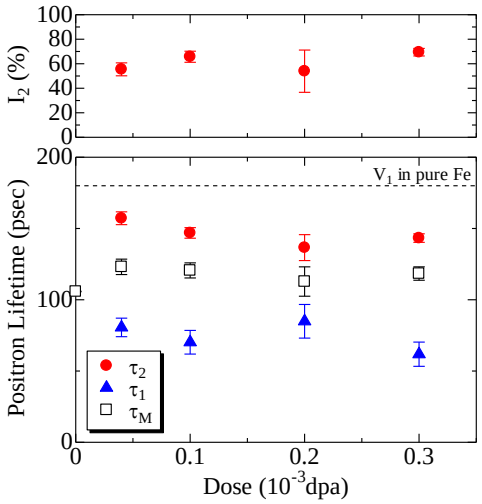

Fig. 1. Changes of the positron lifetime results with dose of electron irradiation of Fe-40Cr alloy

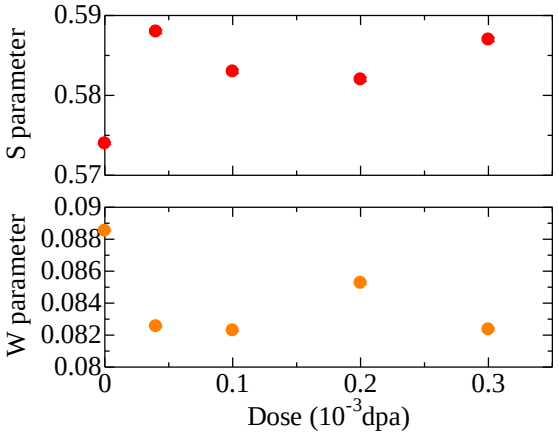

Fig. 2. Changes of the S and the W parameters with dose of electron irradiation of Fe-40Cr alloy

REFERENCE:

[1] K. Okano *et al.*, Nucl. Instr. and Meth., **186** (1981) 115-120.

Thermal Stability of Diamond-like Carbon Films

S. Nakao, X. Qu[1], A. Yabuuchi[1] and A. Kinomura[1]

Structure Materials Research Institute, National Institute of Advanced Industrial Science and Technology
[1]Research Reactor Institute, Kyoto University

INTRODUCTION: Diamond-like carbon (DLC) films have attracted much attention because of their excellent mechanical properties, such as high hardness, high wear resistance and low friction coefficients. However, the thermal stability is relatively low. It is reported that the properties of some films start to be degraded over 200 °C [1]. Therefore, it is important to improve the thermal stability of the films for industrial applications. It is considered that the changes of the microstructure at high temperature should be responsible for the degradation of the properties. The structural changes are related to H desorption and behavior of defects at high temperature. Many studies have been carried out on the thermal stability of DLC films for the purpose of practical use. However, the principal phenomena, such as defect behavior, are not always clear. In addition, many types of DLC or carbon films are presented depending on preparation conditions and methods. Recently, DLC or carbon films are categorized from type I to VI, which includes graphite-like carbon (GLC) and polymer-like carbon (PLC). Therefore, to make clear thermal stability of DLC or carbon films, the examination of every type of DLC films (type I to VI) are necessary. The aim of this study is to clarify the relationship between thermal stability and the behavior of defects and bonded hydrogen in several types of DLC films by positron annihilation and thermal desorption (TDS) method.

EXPERIMENTS: In the first attempt, two types of DLC films (type I and IV) are examined by TDS measurements. DLC films of type I, tetrahedral amorphous carbon (ta-C), are prepared by arc ion plating (AIP) method at Nippon ITF Inc. On the other hand, DLC films of type IV, hydrogenated amorphous carbon (a-C:H), are prepared by bipolar-type plasma based ion implantation (PBII) at AIST-Chubu. The details on PBII system are reported elsewhere [2]. Both films are about 0.5μm in thickness. Si wafer is used as substrate. The TDS spectra of Si substrate are also measured for comparison. The samples are thermally annealed from room temperature to approximately 600 °C. H, H_2, D and DH are detected.

RESULTS: Figure 1 shows the results of H (upper) and H_2 (lower) desorption spectra at elevated temperature. For the sample of AIP (sample A), no significant increase of H and H_2 intensity is observed in the range of 600 °C. The sample A is similar in spectrum of Si substrate (Ref). This shows that the sample A includes quite less hydrogen. On the other hand, a clear peak around 400 °C appears in each H and H_2 desorption spectra for the sample of PBII (sample B). This result clearly shows that hydrogen is released from DLC films over 400 °C for the sample B. It is suggested that thermal stability of sample B is less than that of sample A. In fact, Raman analysis reveals that the structural changes are occurred for the sample B but not for the sample A in the case of 500 °C annealing in vacuum. There is possibility that the structural changes of sample B may be driven by the creation and annihilation of vacancy and defects caused by hydrogen desorption. Positron annihilation measurements will be planned next time.

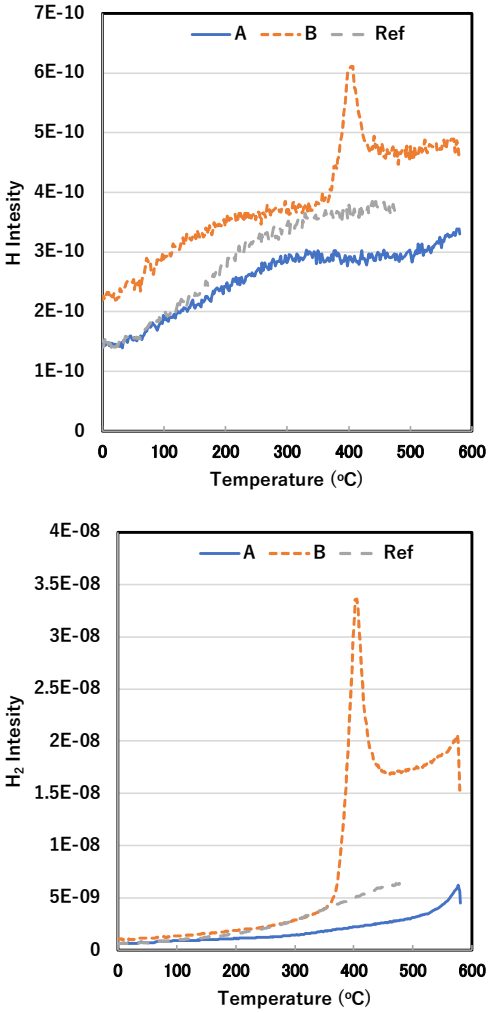

Fig.1 TDS spectra of H and H_2 of DLC films (samples A and B) deposited on Si substrates as a function of annealing temperature. The spectrum of Si substrate is indicated as Ref for comparison.

REFERENCES:

[1] J. Robertson, Mater. Sci. Eng., **R7** (2002) 129-281.
[2] S. Miyagawa *et al.*, Surf. Coat. Technol., **156** (2002) 322-327.